



Voyagaki, E., Crispin, J. J., Gilder, C., Ntassiou, K., O'Riordan, N., Nowak, P., Sadek, T., Patel, D., Mylonakis, G., & Vardanega, P. J. (2021). The DINGO database of axial pile load tests for the UK: settlement prediction in fine-grained soils. *Georisk: Assessment and Management of Risk for Engineered Systems and Geohazards*.
<https://doi.org/10.1080/17499518.2021.1971249>

Publisher's PDF, also known as Version of record

License (if available):
CC BY

Link to published version (if available):
[10.1080/17499518.2021.1971249](https://doi.org/10.1080/17499518.2021.1971249)

[Link to publication record in Explore Bristol Research](#)
PDF-document

This is the final published version of the article (version of record). It first appeared online via Taylor and Francis at <https://doi.org/10.1080/17499518.2021.1971249> . Please refer to any applicable terms of use of the publisher.

University of Bristol - Explore Bristol Research

General rights

This document is made available in accordance with publisher policies. Please cite only the published version using the reference above. Full terms of use are available:
<http://www.bristol.ac.uk/red/research-policy/pure/user-guides/ebr-terms/>

ONLINE SUPPLEMENT

The DINGO Database of Axial Pile Load Tests for the UK: Settlement prediction in fine-grained soils

E. Voyagaki, J. J. Crispin, C. E. L. Gilder, K. Ntassiou, N. O’Riordan, P. Nowak, T. Sadek, D. Patel, G. Mylonakis and P. J. Vardanega

Part A: Supplementary Predicted vs Measured Pile Head Settlement Plots & Discussion

Pile Young’s Modulus

With reference to pile Young’s modulus for bored piles, E_p values as low as 21 *GPa* (Whitaker & Cooke 1966) and as high as 50 *GPa* (Fleming 1992) have been reported. Given the lack of information for the sites at hand and as a first approximation, a value of 30 *GPa*, as used by Fleming (1992), has been adopted for the analysis. Figure S1 shows the database analysed for a factor of safety of 2.5 with E_p varying from 20 *GPa* to 40 *GPa*. Naturally, predicted displacements tend to get smaller with increasing E_p , which leads to points gradually shifting to the left of the graphs (no variation in the vertical axis as measured values are not altered). The main trends identified in the previous figures are the same for all values of E_p . The influence of E_p on the initial head stiffness can be assessed from the dimensionally homogeneous expression in Eq. S1:

$$K_{el} = \chi_1 (E_p)^{\chi_2} (E_s)^{1-\chi_2} D_s \quad (S1)$$

where χ_1, χ_2 are dimensionless coefficients.

From Winkler theory (Mylonakis 1995, 2001), $\chi_2 = 1/2$. For very short piles ($L/D_s < 5$), χ_1 is approximately proportional to $(E_p/E_s)^{-1/2}$ whereas for very long piles ($L/D_s > 50$) χ_1 is practically independent of (E_p/E_s) . Accordingly, K_{el} is independent of E_p for short piles and proportional to $(E_p)^{1/2}$ for long piles. In this light, for very long piles an increase in E_p from 30 *GPa* to, say, 40 *GPa* would lead to a maximum reduction in elastic pile settlement of approximately $(30/40)^{0.5} \approx 0.87$ that is a 13% reduction. For shorter piles such as those examined herein, the reduction will naturally be smaller. Evidently, this minor effect explains the stability of the main trends across all graphs in Figure S1.

a-value

Following Skempton (1959), Poulos & Davis (1980), Fleming *et al.* (2009), Patel (1992) and LDSA (2017), $\alpha = 0.5$ can be considered an acceptable design value for piles in London clay. As limited information is available outside London and most tests in the database were not carried out to failure (nor is the definition of failure the focus of this study), the same α value was applied to all deposits. Given that many of the tests in the database have not been carried to failure the computation of the factor of safety (F) is reliant on the calculated pile capacities (which is obviously reliant on all the strength parameters involved). That said even if one had all the pile tests complete the definition of failure of a single pile test is somewhat arbitrary e.g. a percentage of pile diameter can be used but other performance criteria could also be sensibly assigned. Figure S2 shows the entire dataset evaluated for $\alpha = 0.4, 0.5$ and 0.6 and relatively little variation is revealed.

Bearing Capacity Factor

Figure S3 shows the effect of varying N_c from 9 to 13. For the analysis in this paper $N_c = 9$ has been adopted in accordance with accepted practice (e.g. Meyerhof, 1976), although lower or higher values of N_c would be used depending on the circumstances e.g. if embedment in the founding strata was not sufficient. As for α the effect of this variation is relatively modest.

Deformation parameters

Deformation parameters were based on the mean values from the database of 17 high-quality tests for London clay, Vardanega and Bolton (2011b). For Model 2, a (G/c_u) value of 320 has been used. Figure S4 shows database analysed with (G/c_u) of 240, 320 and 400 and the effect is also relatively modest. For Model 1 values of $\gamma_{M=2}$ and b are needed (Figure 3); a sensitivity study for the early variant of model one is presented in Vardanega (2015). Following the aforementioned publications, the average value of $\gamma_{M=2}$ of 7×10^{-3} and b of 0.6 have been applied (these values are also similar to the average values for a larger database of tests on fine-grained soils, Vardanega and Bolton 2011a). Figure S5 shows the

database analysed using $\gamma_{M=2}$ of 5×10^{-3} , 7×10^{-3} , and 9×10^{-3} (plus or minus the standard deviation value used in Vardanega 2015) and the effect is again not significant. Figure S6 shows the database analysed using $\gamma_{M=2}$ of 0.48, 0.6, 0.72 (plus or minus the standard deviation value used in Vardanega 2015). The influence of this soil ductility parameter (as also shown in Vardanega 2015) is more significant. To measure b for a specific site, high-quality triaxial testing is needed. However, the value $b = 0.6$ for natural clays is supported by a relatively large database (Vardanega and Bolton 2011a).

Figures S7 – S10 are equivalent to Figures 7 – 10 in the main text, showing all data points (even beyond $w_0/D_b = 1\%$). Figures S11a (data points up to $w_0/D_b = 1\%$) and S11b (all data) show results for the epoch of the tests, grouped in six decades starting from the 1950's and going post 2000. No clear difference in the quality of the settlement predictions is observed between 'old' and 'new' field tests, with a tendency for somewhat conservative predictions from both methods been apparent in all graphs, especially at low loads. The absence of this trend in some of the subsets (e.g. in the 1950's and 1990's, involving only 25 cases in total) may simply be coincidental. Figures S12 – S13 are equivalent to Figures 12 & 13 in the main text, showing all data points.

References

- Fleming, W.G.K. (1992). A new method for single pile settlement prediction and analysis. *Géotechnique*, **42**(3), 411-425. <https://doi.org/10.1680/geot.1992.42.3.411>
- Fleming, W.G.K., Weltman, A.J., Randolph, M.F. & Elson, W.K. (2009). *Piling Engineering*, 3rd edition. Wiley, New York, NY, USA.
- London District Surveyors Association (LDSA) (2017). *Foundations no. 1: Guidance notes for the design of straight shafted bored piles in London clay*. London, UK.
- Meyerhof, G.G. (1976). Bearing capacity and settlement of pile foundations (11th Terzaghi Lecture). *Journal of the Geotechnical Engineering Division (American Society of Civil Engineers)* **102**(3), 195–228.
- Mylonakis, G. (1995). *Contributions to Static and Seismic Analysis of Piles and Pile-Supported Bridge Piers*. PhD Thesis, State University of New York at Buffalo.
- Mylonakis, G. (2001). Winkler modulus for axially loaded piles. *Géotechnique*, **51**(5), 455-461. <https://doi.org/10.1680/geot.2001.51.5.455>
- Patel, D.C. (1992). Interpretation of results of pile tests in London clay. *Piling Europe*, Thomas Telford, London, UK.
- Poulos, H.G. & Davis, E.H. (1980). *Pile Foundation Analysis & Design*. Wiley.
- Skempton, A.W. (1959). Cast-in-situ bored piles in London clay. *Géotechnique*, **9**(4), 153-173. <https://doi.org/10.1680/geot.1959.9.4.153>.
- Vardanega, P.J. (2015). Sensitivity of simplified pile settlement calculations to parameter variation in stiff clay. In: *Geotechnical Engineering for Infrastructure and Development* (Winter, M.G. et. al. (eds.)). ICE Publishing, London, United Kingdom, vol. 7, pp. 3777-3782.
- Vardanega, P.J. & Bolton, M.D. (2011a). Strength mobilization in clays and silts. *Canadian Geotechnical Journal*, **48**(10), 1485-1503, <http://doi.org/10.1139/T11-052> and Corrigendum, **49**(5), 631, <http://doi.org/10.1139/t2012-023>

- Vardanega, P.J. & Bolton, M.D. (2011b). Predicting Shear Strength Mobilisation of London Clay. *Proceedings 15th European Conference on Soil Mechanics and Geotechnical Engineering: Geotechnics of Hard Soils – Weak Rocks*, (A. Anagnostopoulos et al. eds.), IOS Press, Amsterdam, The Netherlands, vol. 1 pp. 487-492, <http://doi.org/10.3233/978-1-60750-801-4-487>
- Whitaker, T. & Cooke, R.W. (1966). An investigation of the shaft and base resistance of large bored piles in London Clay. In: *Large Bored Piles: Proceedings of the Symposium by the Institution of Civil Engineers and the Reinforced Concrete Association; Institution of Civil Engineers*, London, UK, 7-49.

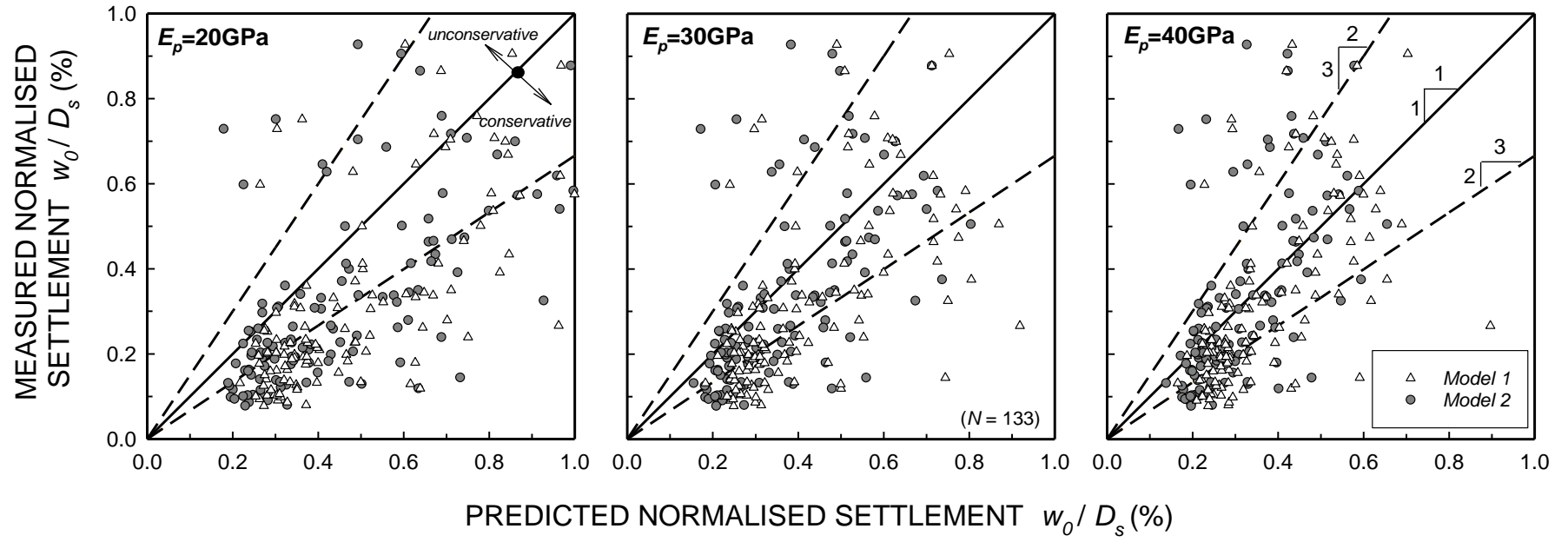


Figure S1. Predicted versus measured pile head settlement plot for different values of pile Young's modulus; Dataset refers to bored piles, cohesive soils, $F_{total} = 2.5$, $\alpha = 0.5$, $N_c = 9$. (Predictions according to Models 1 and 2.)

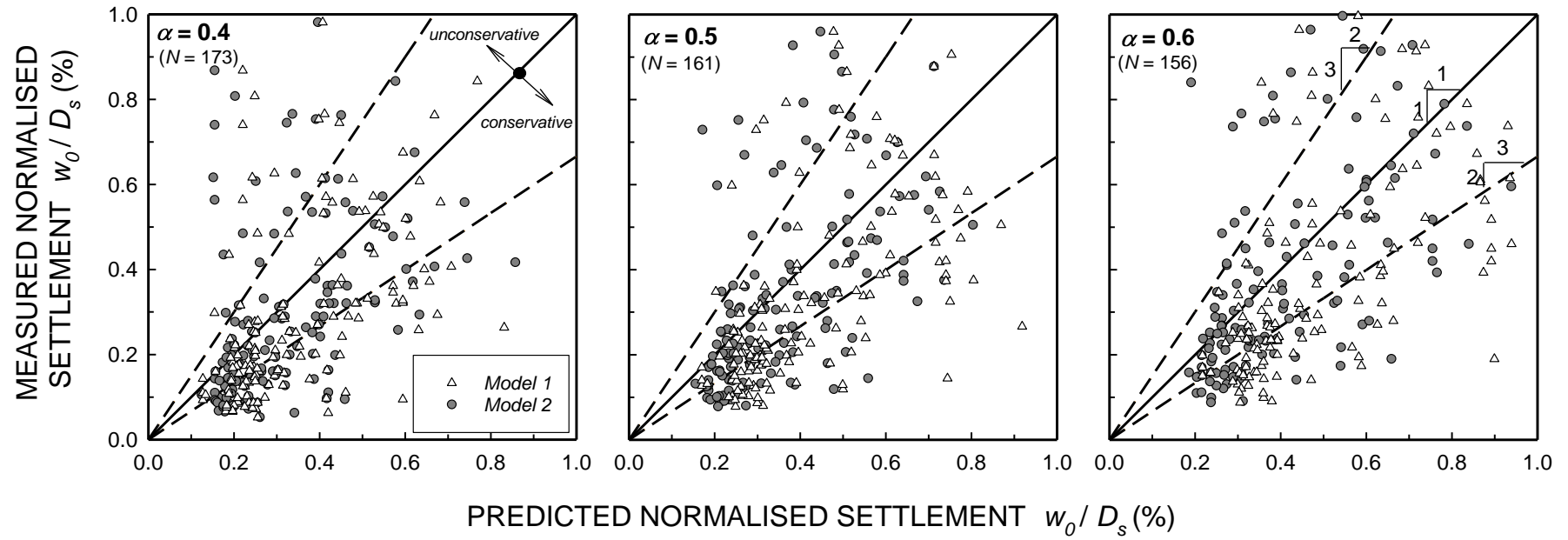


Figure S2. Predicted versus measured pile head settlement plot for different values of the α value: cohesive soils, $F_{total} = 2.5$, $N_c = 9$. (Predictions according to Models 1 and 2.) For bored piles, $E_p = 30 \text{ GPa}$

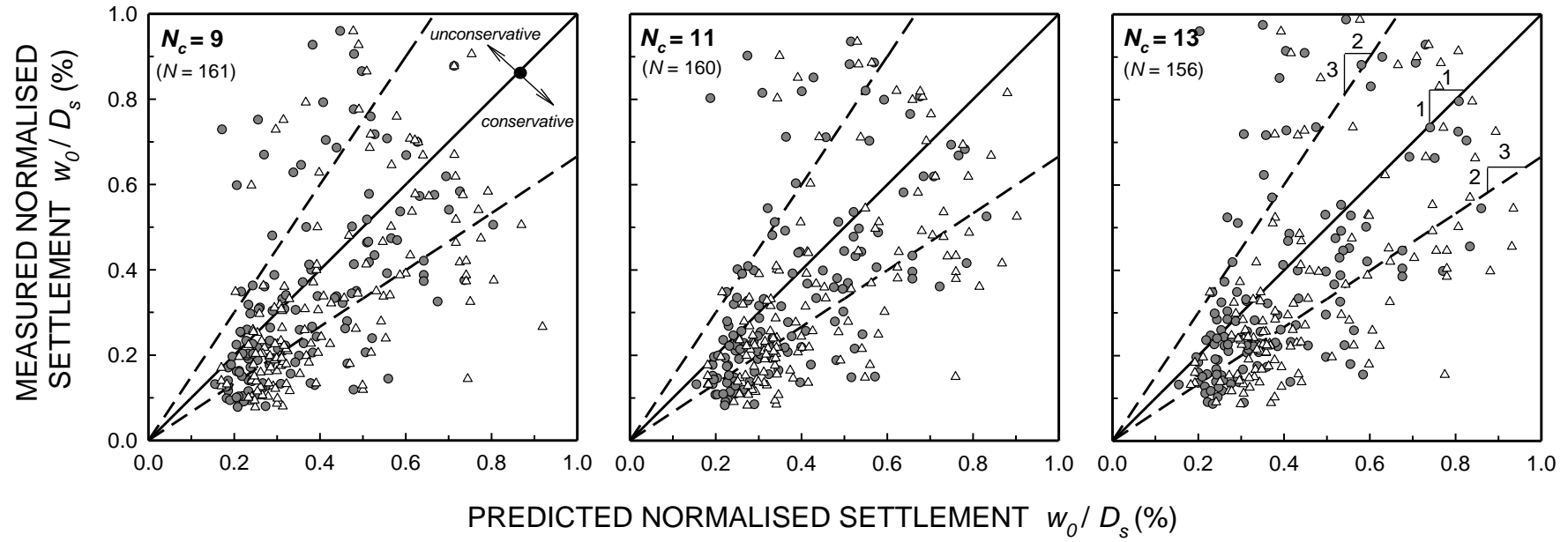


Figure S3. Predicted versus Measured pile head settlement plot for different values of tip bearing capacity coefficient: cohesive soils, $F_{total} = 2.5$, $\alpha = 0.5$. (Predictions according to Models 1 and 2.) For bored piles, $E_p = 30 \text{ GPa}$

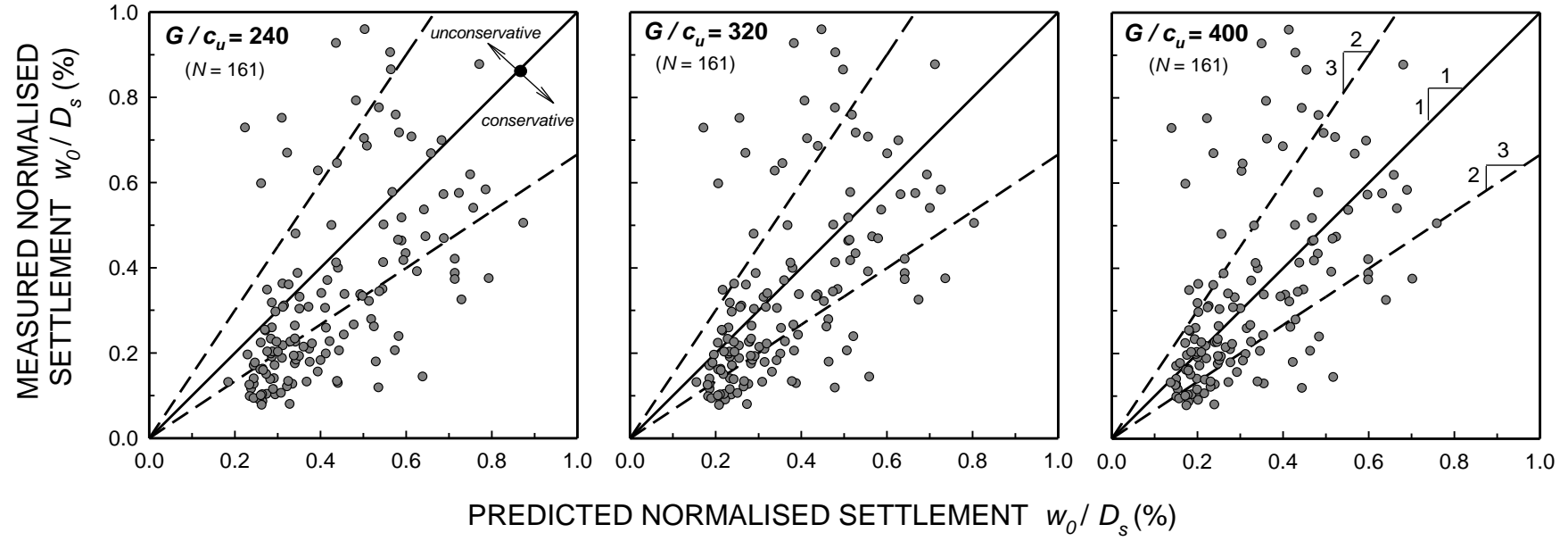


Figure S4. Predicted versus Measured pile head settlement plot for different values of G/c_u : cohesive soils, $F_{total} = 2.5$, $\alpha = 0.5$, $N_c = 9$. (Predictions according to Model 2.) For bored piles, $E_p = 30 \text{ GPa}$

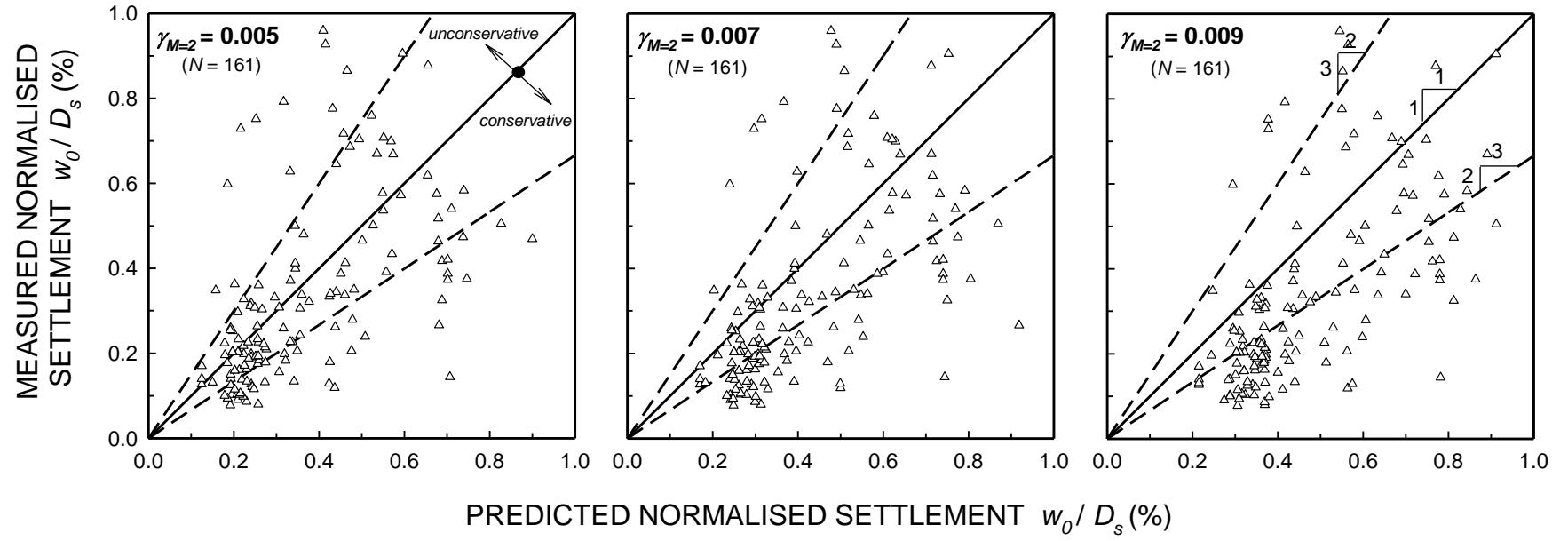


Figure S5. Predicted versus Measured pile head settlement plot for different values of $\gamma_{M=2}$: cohesive soils, $F_{total} = 2.5$, $\alpha = 0.5$, $N_c = 9$. (Predictions according to Model 1.) For bored piles, $E_p = 30 \text{ GPa}$

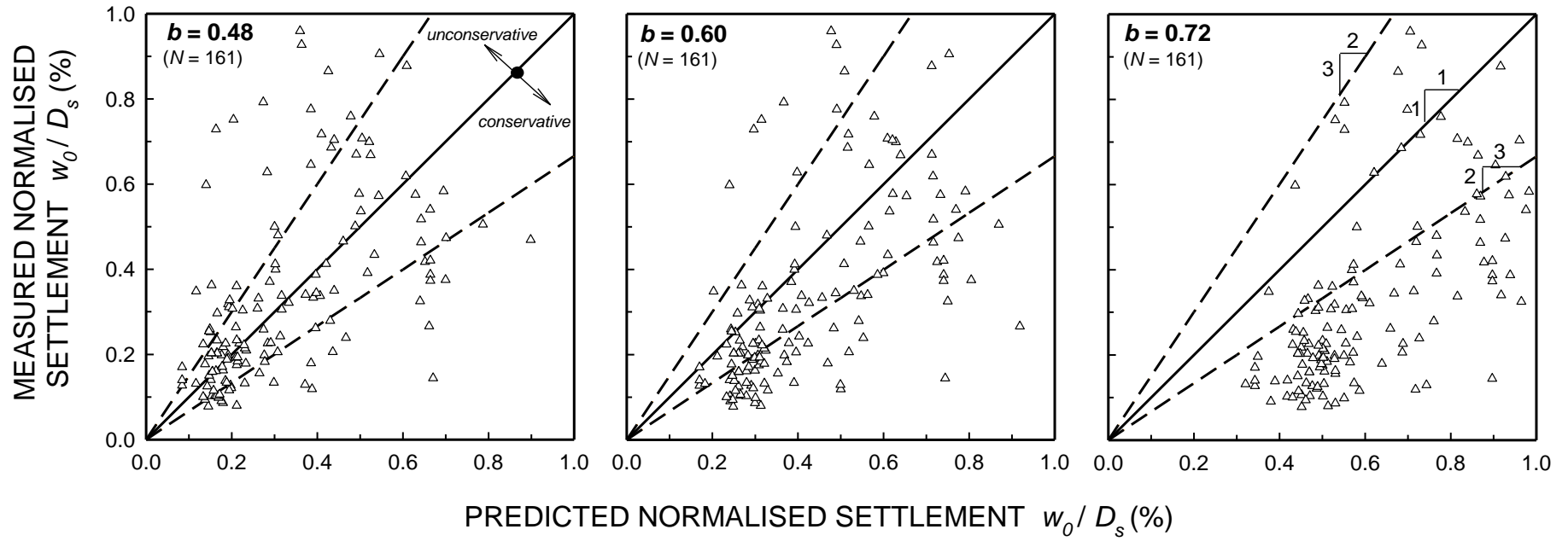


Figure S6. Predicted versus Measured pile head settlement plot for different values of b : cohesive soils, $F_{total} = 2.5$, $\alpha = 0.5$, $N_c = 9$. (Predictions according to Model 1) For bored piles, $E_p = 30 \text{ GP}$

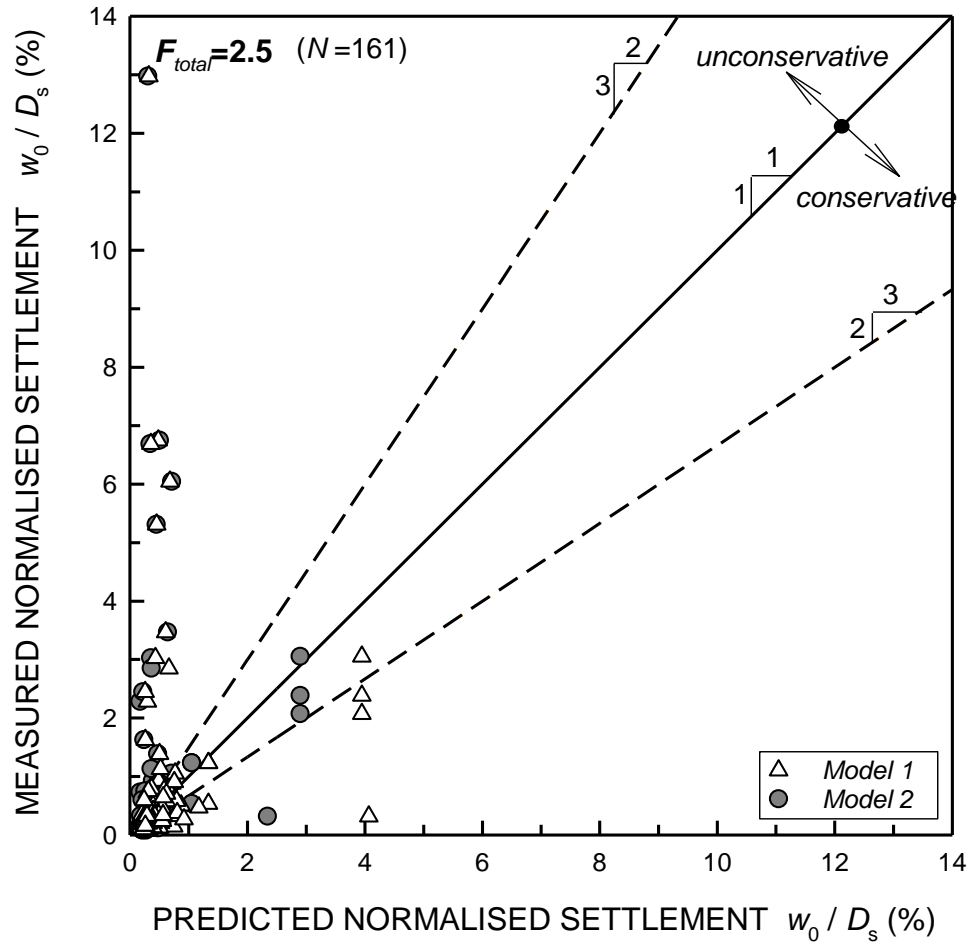


Figure S7. Predicted versus measured pile head settlement plot for the full set of data analysed in this study (model parameters from Table 2).

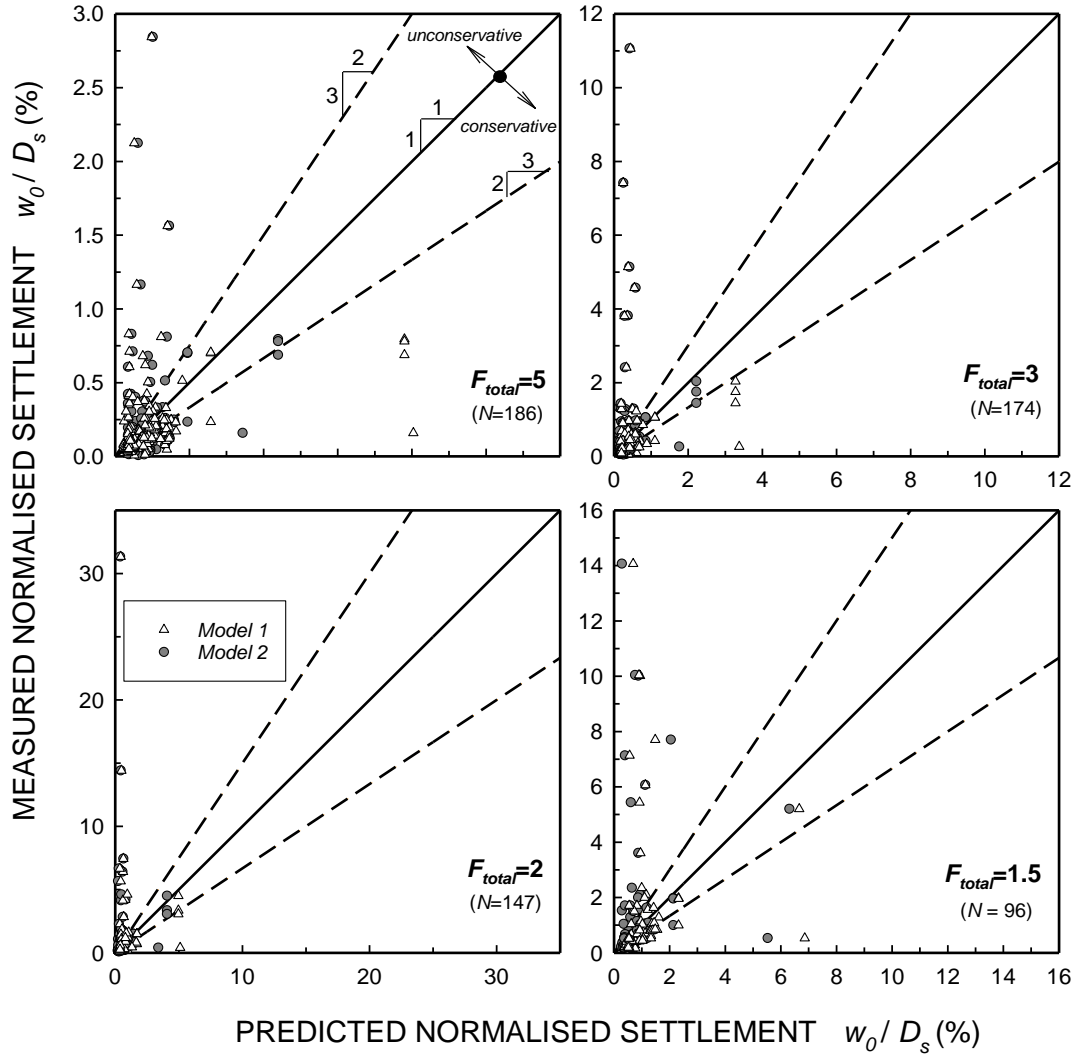


Figure S8. Predicted versus measured pile head settlement plot for different values of factors of safety for the full set of data analysed in this study (model parameters from Table 2).

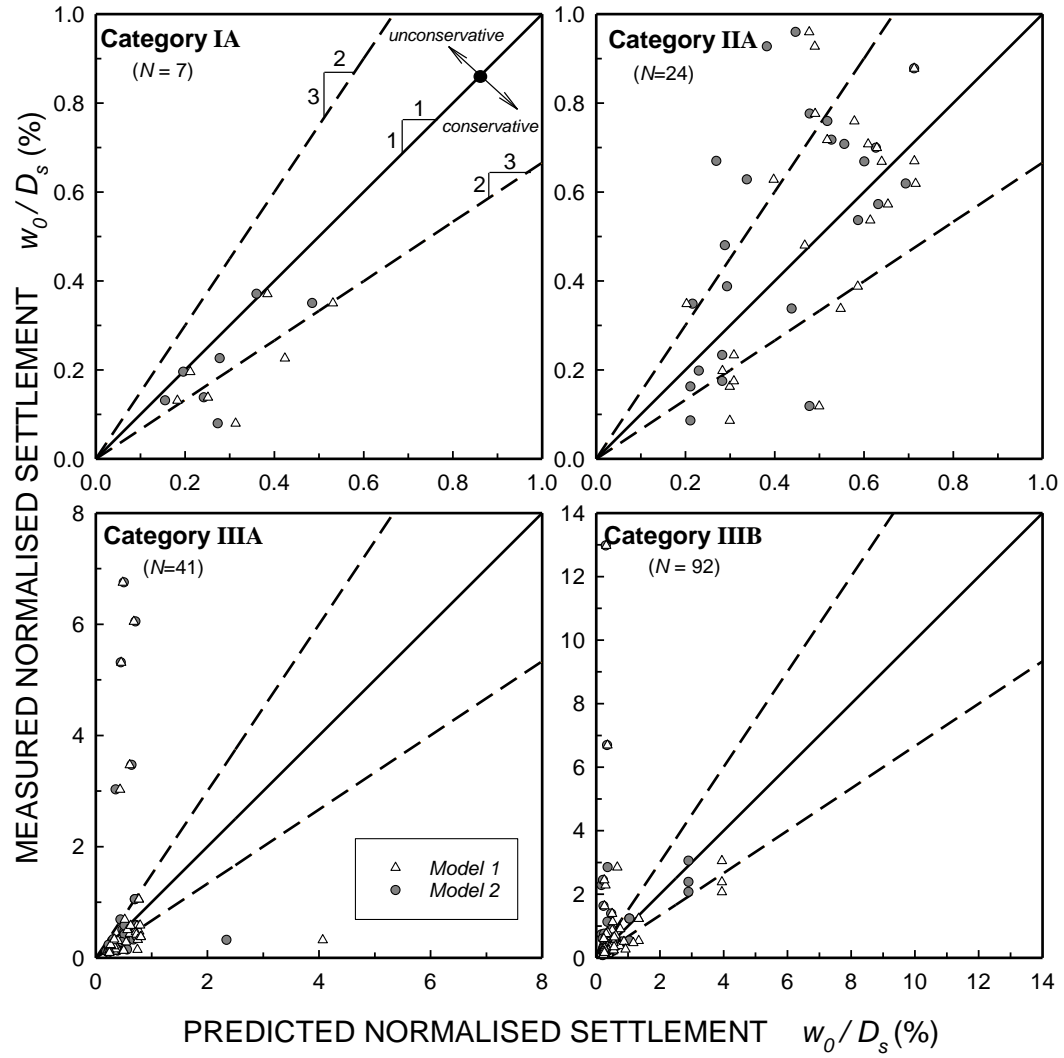


Figure S9. Predicted versus measured pile head settlement plot organised by soil parameter source (categories described in Table 3, model parameters from Table 2)

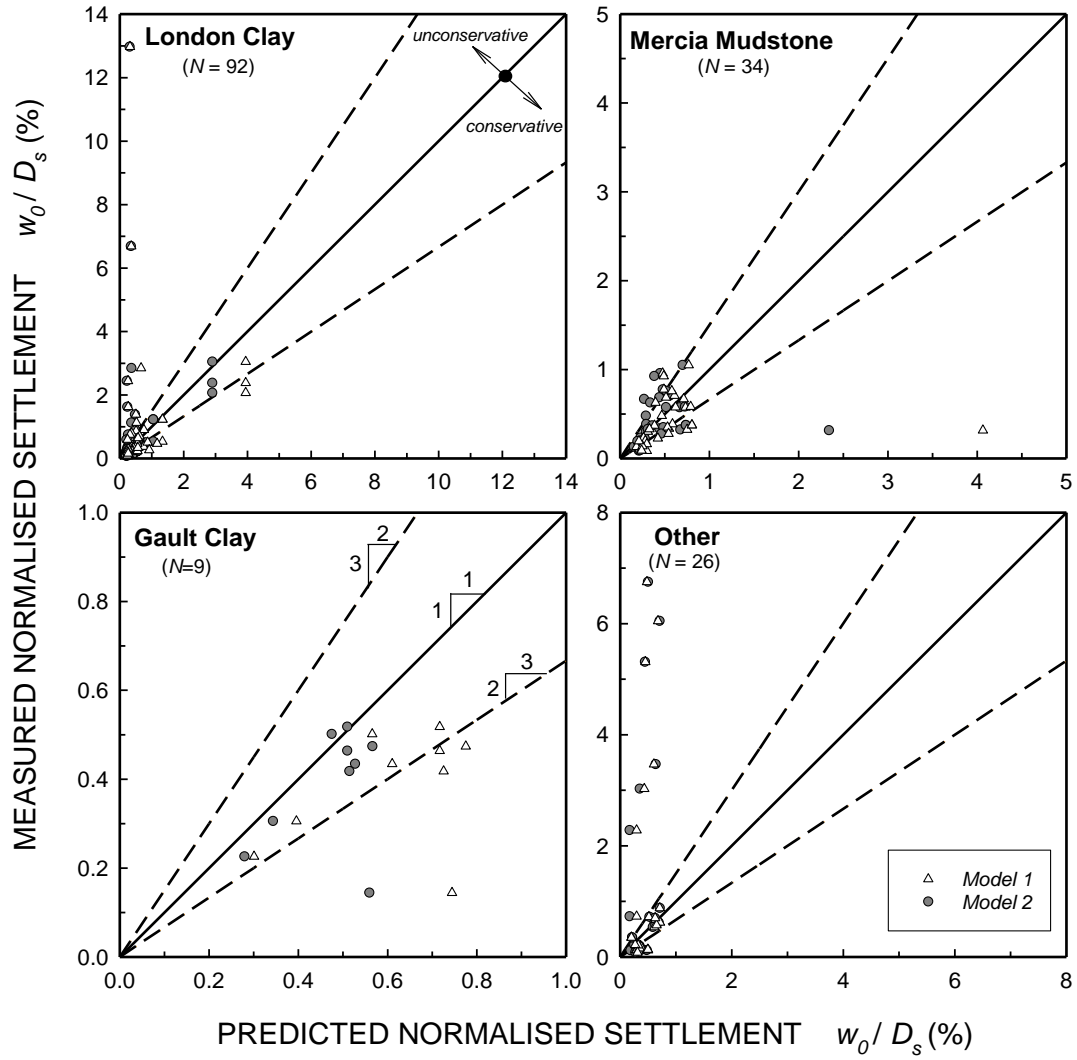


Figure S10. Predicted versus measured pile head settlement plot organised by soil type (parameters from Table 2)

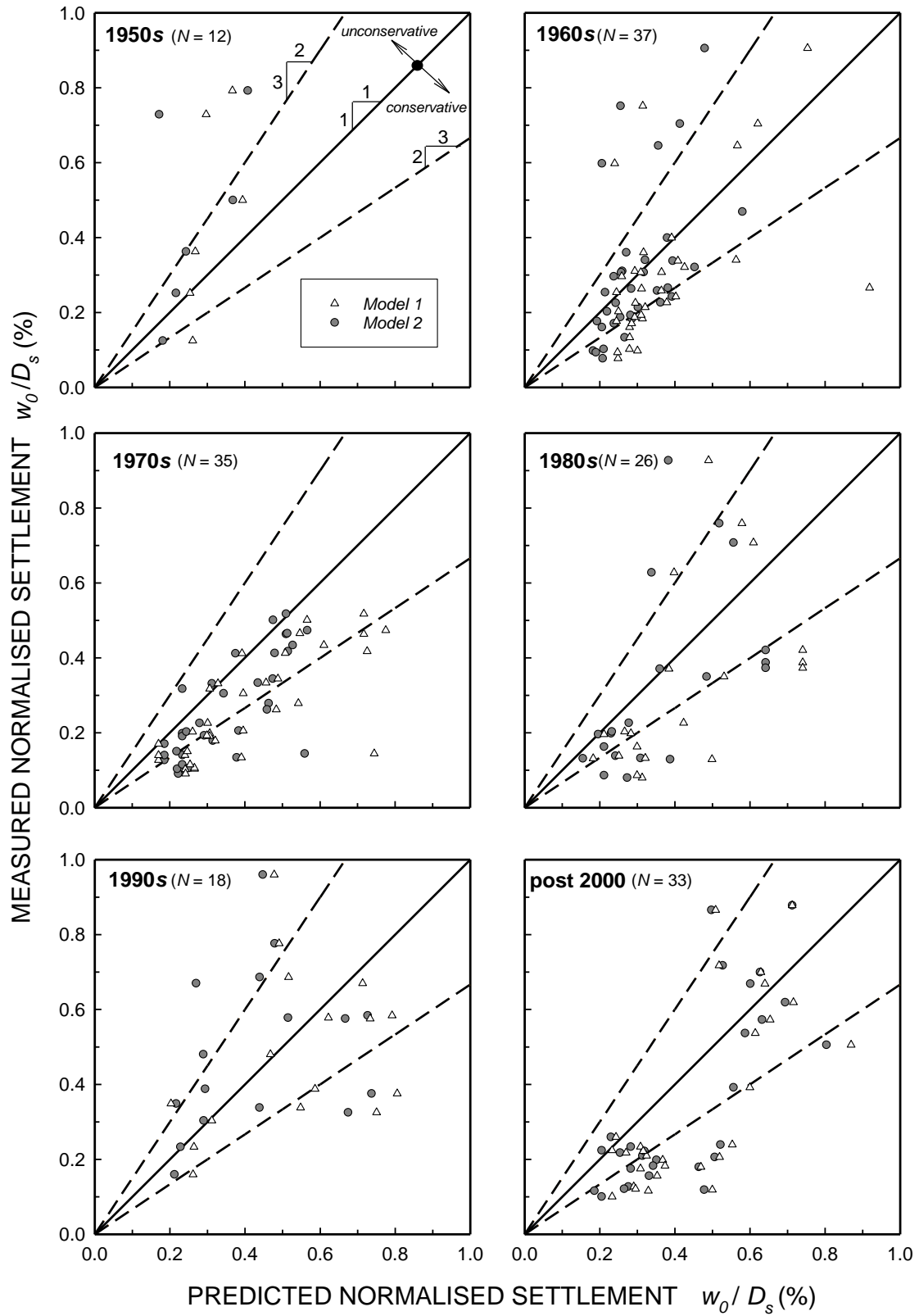


Figure S11a. Predicted versus measured pile head settlement plot organised by epoch of the tests (parameters from Table 2; data shown up to $w_o/D_b = 1\%$).

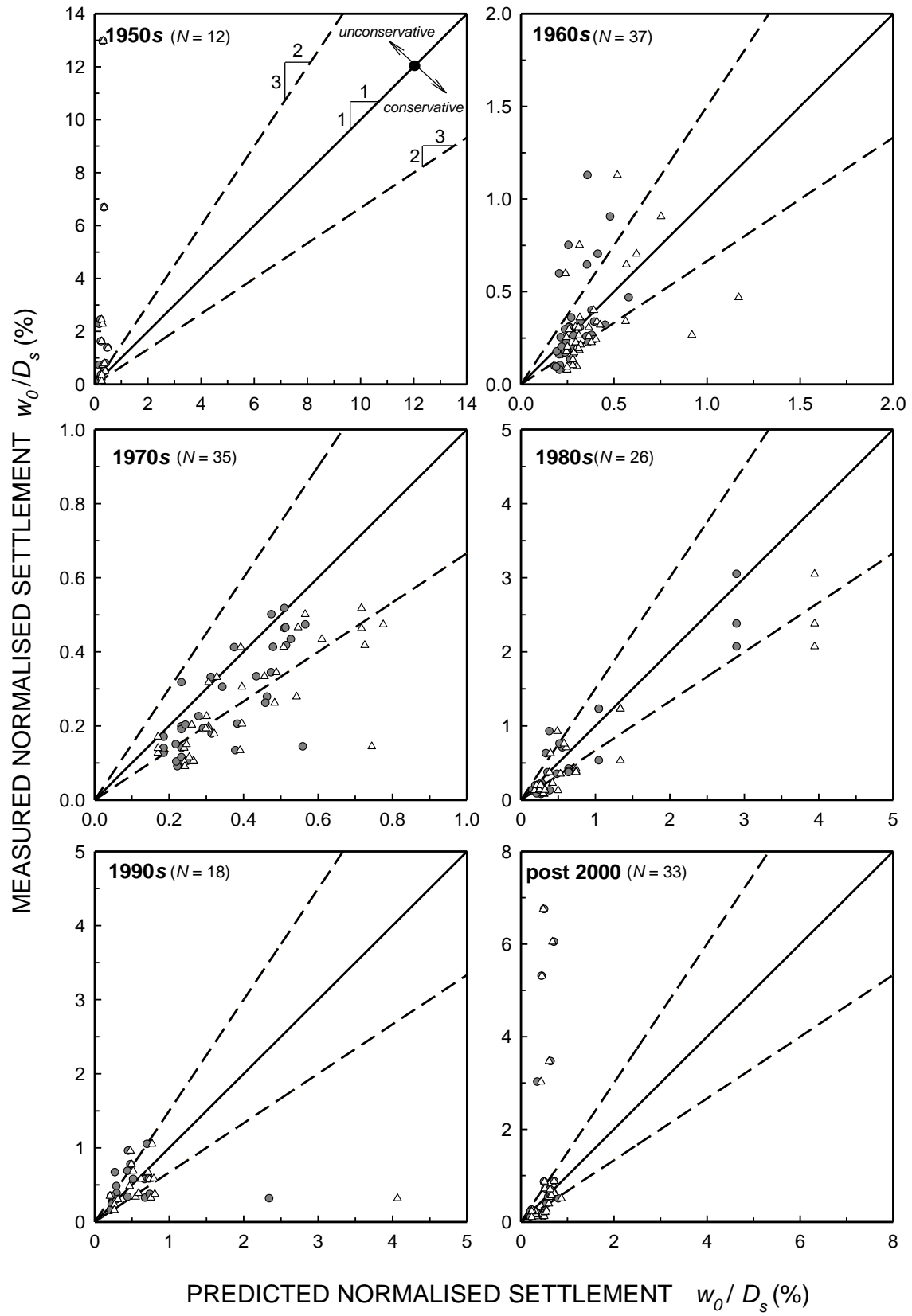


Figure S11b. Predicted versus measured pile head settlement plot organised by epoch of the tests (parameters from Table 2).

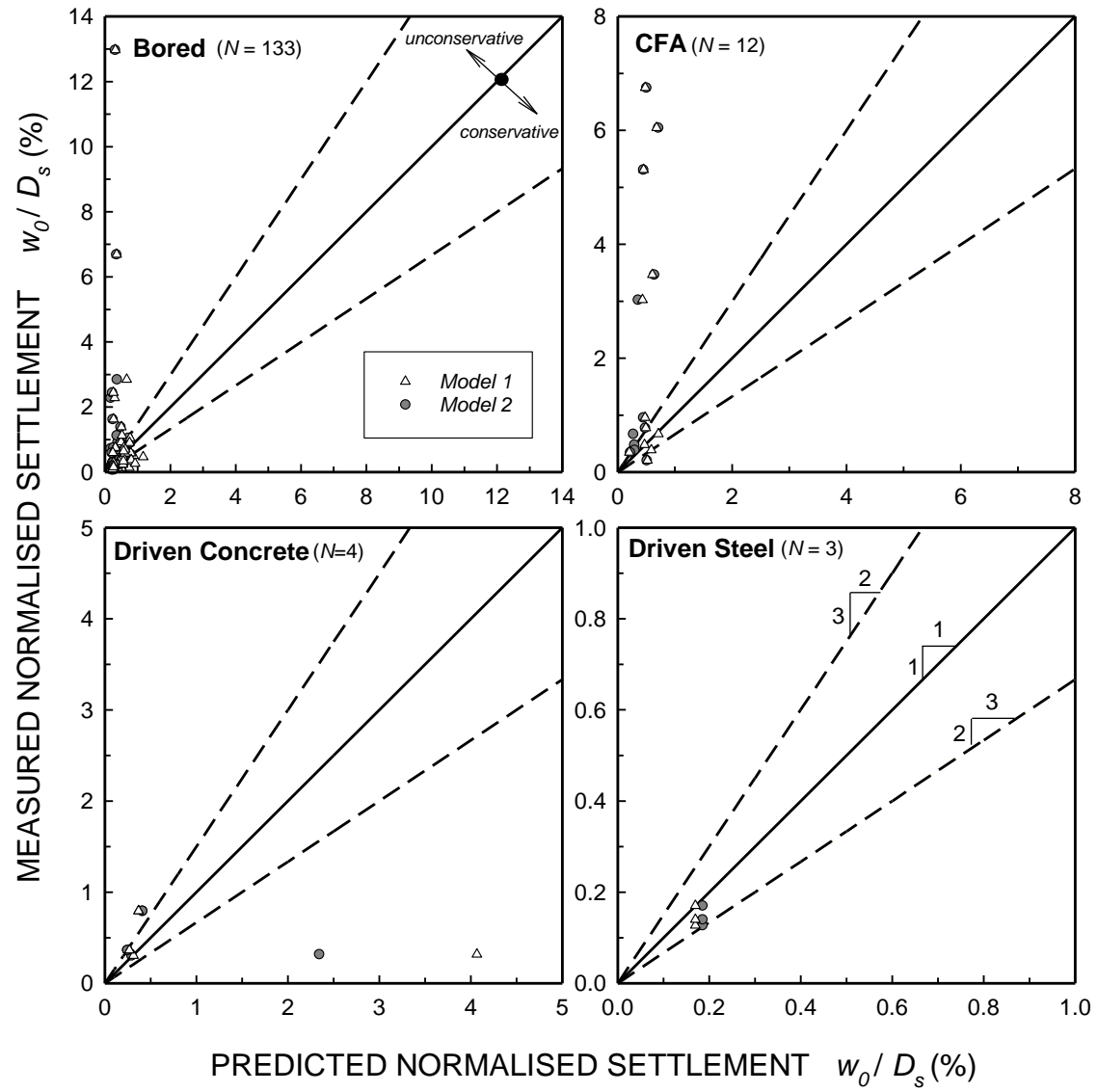


Figure S12. Predicted versus measured pile head settlement plot organised by construction method (parameters from Table 2)

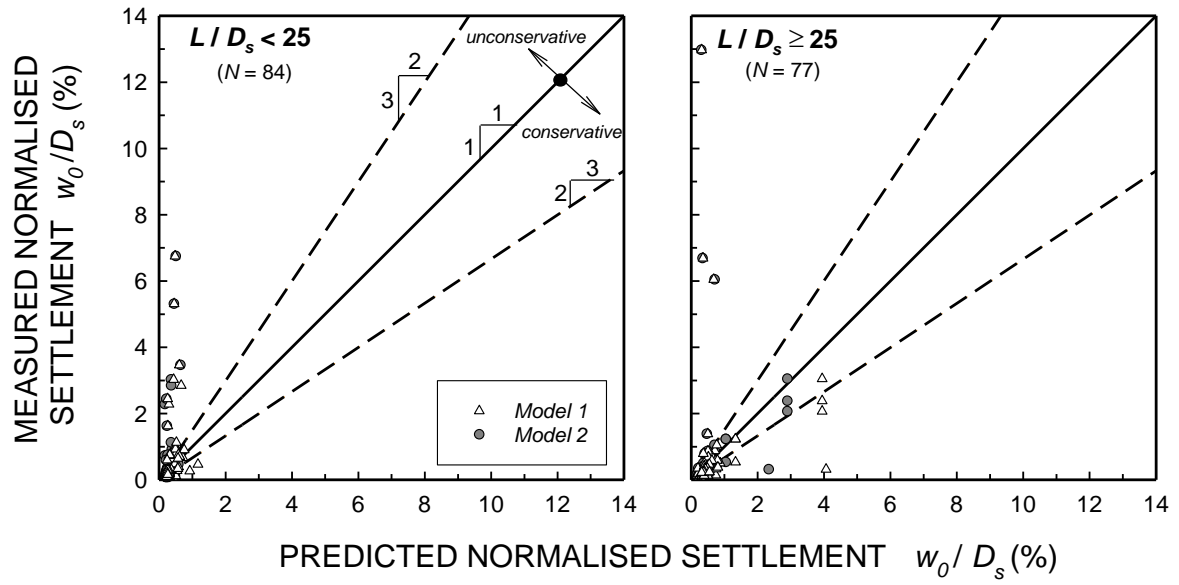


Figure S13. Predicted versus measured pile head settlement organised by pile slenderness (parameters from Table 2)

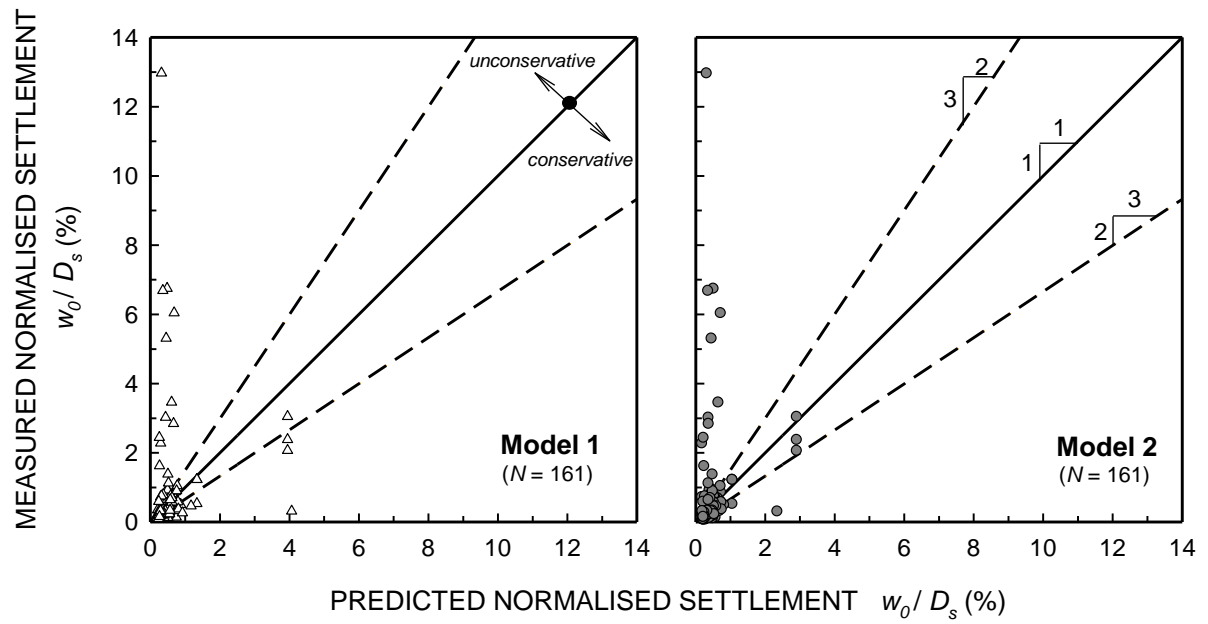


Figure S14. Predicted versus measured pile head settlement comparing Model 1 and Model 2 (parameters from Table 2)

Part B: Full list of load-settlement curves employed in the presented analyses

A row of plots is included for each pile analysed. The DINGO site and pile ID is included on the left of each row. Four plots are included for each pile:

The first plot shows the load-settlement curves for the pile. If multiple tests were carried out on one pile, then multiple measured lines are included with a legend that indicates the PTST_ID from the DINGO database. Predictions are shown for both models considered in this paper.

The second plot shows a geological cross section of the geology the pile is installed in. The pile construction method and dimensions are indicated along with a basic cross section showing the shape of the pile. The soil deposits are coloured according to the geology code assigned and hatched according to the soil descriptions. A legend is provided in Figure S15 with these codes.

The third plot shows the design undrained shear strength line selected for the pile analysis.

The fourth plot shows the calculated Winkler spring stiffness and strength per unit length.

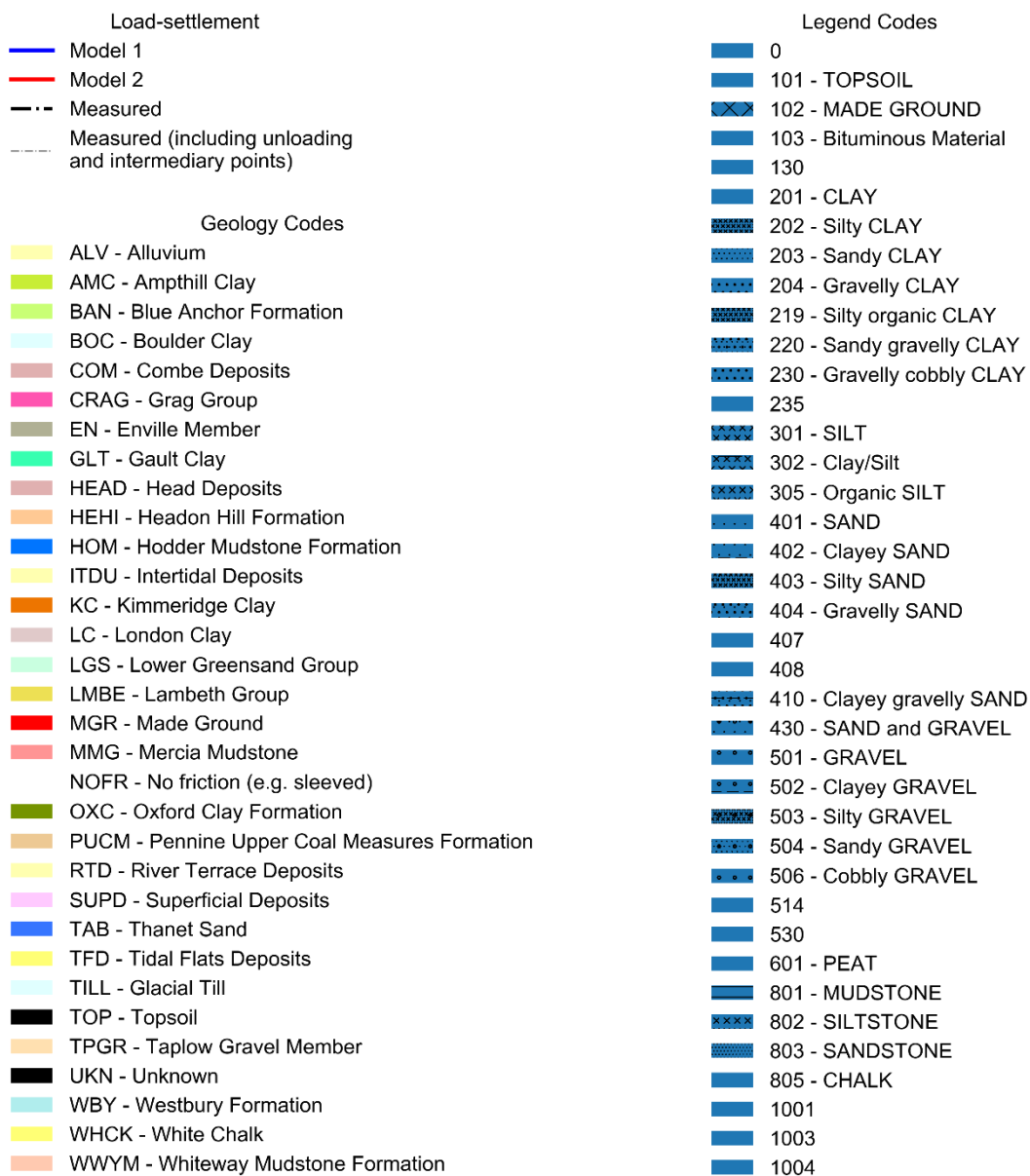


Figure S15. Legend for load-settlement curves and geological cross sections

